ARTICLE

Ultrasensitive and Highly Selective Detection of Alzheimer's Disease Biomarker Using Two-Photon Rayleigh Scattering Properties of Gold Nanoparticle

Adria Neely, Candice Perry, Birsen Varisli, Anant K. Singh, Tahir Arbneshi, Dulal Senapati, Jhansi Rani Kalluri, and Paresh Chandra Ray*

Department of Chemistry, Jackson State University, Jackson, Mississippi

ABSTRACT Alzheimer's disease (AD) is a progressive mental disorder disease, which affects 26.6 million people worldwide and estimated increments can be 100 millions by 2050. Since there is no cure at present, early diagnosis of AD is crucial for the current drug treatments. Driven by the need, here we demonstrate for the first time that monoclonal anti-tau antibody-coated gold nanoparticle based two-photon scattering assay can be used for the detection of Alzheimer's tau protein in the 1 pg/mL level which is about 2 orders of magnitude lower than cutoff values (195 pg/mL) for tau protein in CSF (cerebrospinal fluid). We have shown that when anti-tau antibody-coated gold nanoparticles were mixed with 20 ng/mL of tau protein, two-photon Rayleigh scattering intensity (TPRS) increases by about 16 times. The mechanism of TPRS intensity change has been discussed. Our data demonstrated that our TPRS assay is highly sensitive to tau protein and it can distinguish from BSA, which is one of the most abundant protein components in CSF. Our results demonstrate the potential for a broad application of this type of nanobionanotechnology in practical biomedical applications.

KEYWORDS: Alzheimer's biomarker · gold nanoparticle · tau protein · two-photon Rayleigh scattering · plasmonics

Alzheimer's disease (AD) is a brain disorder disease that destroys brain cells, causing problems with long-term memory loss, irritability, aggression, and mood swings.[1−3] There were 26.6 million people suffering from Alzheimer's disease worldwide in 2006, and this number is expected to increase 4 times (<100 million) by 2050.[1−9] Despite the huge problems, there is no definitive diagnosis of AD, other than postmortem identification of senile plaques and neurofibrillary tangles in the brain tissue. Neurofibrillary tangles are insoluble twisted fibers formed because of hyperphosphorylated tau protein aggregation in brain cells. Tau proteins play a very important role in the structure of the neuron. In AD patient's CSF (cerebrospinal fluid), tau protein is phosphorylated at more than 20 residues. These phosphorylated tau proteins bind to each other inside nerve cells, tying themselves in "knots" known as NFTs.[1−9] Recently it has been shown[1−9] that patients with Alzheimer's dementia have much higher hyperphosphorylated tau protein in CSF compared to control groups. As a result, ultrasensitive methods for measurement of the level total tau can provide an opportunity to develop clinical lab diagnostic for AD. Since there is no cure at present, early diagnosis of AD is crucial for the current drug treatments, which have shown to slow the progression of AD. Driven by the growing market needs of the 21st century, this paper reports the development of gold nanomaterial-based two-photon Rayleigh scattering (TPRS) assay for the ultrasensitive and selective detection of tau protein AD biomarker. Two-photon scattering properties have been monitored using the hyper−Rayleigh scattering (HRS) technique.[10−18] This technique can be easily applied to study a very wide range of materials because electrostatic fields and phase matching are not required. Other advantages are that the polarization analysis gives information about the tensor properties, and spectral analysis of the scattered light gives information about the dynamics.

In the last 15 years, the field of biosensor using nanomaterial has witnessed an explosion of interest in the use of nanomaterials in assays for DNA/RNA, protein, and cell markers for many diseases.[19−34] The integration of nanotechnology with biology and medicine is expected to produce major advances in molecular diagnostics, therapeutics, and bioengineering.[19−44] In

*Address correspondence to paresh.c.ray@jsums.edu.

Received for review July 16, 2009 and accepted August 13, 2009.

Published online August 19, 2009.
10.1021/nn900813b CCC: $40.75

terms of biological sensing, the use of nanotechnology has led to the production of numerous, rapid, sensitive multianalytes assays which are useful not only in the laboratory, but also in the field as portable instruments.[29−45] Because of the increasing availability of nanostructures with highly controlled optical properties, nanosystems are attractive in their use in biotechnological systems for diagnostic application. Gold nanosystems are attractive because of their unique properties, including their shape and size-dependent optical properties. Owing to the lack of toxicity,[12−45] scientists have shown great interest in using gold nanosystems for biomarker applications and biological imaging. Mirkin *et al.*[6,8] and others[28,29] have demonstrated that nanoparticle-based biobarcode assays with localized surface plasmon resonance (LSPR) are capable of measuring the ADDL level in CSF. Here, we demonstrate for the first time that monoclonal anti-tau antibody (tau-mab) coated gold nanoparticle based two-photon scattering assay[10−18,46,47] can be used for the detection of Alzheimer's tau protein at the 1 pg/mL level, which is about 2 orders of magnitude lower than cutoff values (195 pg/mL) for tau protein in CSF. Our results reported here demonstrate the potential for a broad application of bioconjugated nanoparticles in practical biotechnological and medical applications.

RESULTS AND DISCUSSION

Our two-photon scattering approach for the detection of selective AD biomarker is based on the fact that, the monoclonal anti-tau antibody-conjugated gold nanoparticles can readily and specifically identify tau protein, through antibody−antigen interaction and recognition (as shown in Figure 1). For a tau protein, there are many surface antigens available for specific recognition with monoclonal anti-tau antibody-conjugated nanoparticles. Therefore, in the presence of tau protein, several nanoparticles can bind to each protein, thereby producing nanoparticle aggregates (as shown in Figure 1). As a result, a colorimetric change has been observed from red to bluish color (as shown in Figure 2) and a new broadband appears around 150 nm far from their plasmon absorption band, as shown in Figure 2B.

As shown in Figure 2C, when monoclonal anti-tau antibody-conjugated gold nanoparticles were mixed with various concentrations of tau protein, two-photon scattering intensity increases by about 16 times (as shown in Figure 2). Our experimental results demonstrated a very distinct two-photon scattering intensity change (2.2 times) even upon the addition of 1 pg/mL tau protein. To evaluate whether our assay is highly selective, we have also performed how two-photon scattering intensity changes upon addition of serum albumin (BSA) protein and heme protein, instead of tau protein with anti-tau-antibody conjugated gold nanoparticles. As shown in Figure 2C, two-photon scattering intenity changes only 1.2 times in presence of 200 ng/mL BSA protein and 1.6 times when we added 30000 ng/mL of BSA protein to monoclonal anti-tau antibody-conjugated gold nanoparticles. Similarly when we added 3000 ng/mL heme protein to monoclonal anti-tau antibody-conjugated gold nanoparticles, two-photon scattering intensity changes only 1.2 times.

Two-photon scattering signal from monoclonal anti-tau antibody-conjugated gold nanoparticles can be expressed as[10−19,45−47]

$$I_{TPRS} = G\langle N_w\beta_w{}^2 + N_{nano}\beta_{nano}{}^2\rangle I_\omega{}^2 \exp(-N_{nano}\varepsilon_{2\omega}l) \quad (1)$$

where G is a geometric factor, N_w and N_{nano} the number of water molecules and monoclonal anti-tau antibody-conjugated gold nanoparticle per unit volume, β_ω and β_{nano} are the quadratic hyperpolarizabilities of a single water molecule and a single monoclonal anti-tau antibody-conjugated gold nanoparticle, $\varepsilon_{2\omega}$ is the molar extinction coefficient of the gold nanoparticle at 2ω, l is the path length, and I_ω is the fundamental intensity. The exponential factor accounts for the losses through absorption at the harmonic frequency. Considering the size of nanoparticle, the approximation that assumes that the electromagnetic fields are spatially constant over the volume of the particle may not be suitable anymore. As a result, the total nonlinear polarization consists of different contributions such as multipolar radiation of the harmonic energy of the excited dipole and possibly of higher multipoles, as we discussed in our previous publication or reported by others.[12−19] The TPRS intensity therefore also consists of several contributions. The first one is the electric dipole approximation, which may arise due to the defects in nanoparticle. This contribution is actually identical to the one observed for any noncentrosymmetrical pointlike objects such as efficient rodlike push−pull molecules.[10,11,45,46] The second contribution is multipolar contribution like electric quadrupole contribution.[12−19] This contribution is very important when the size of the particle is no longer negligible when compared to the wavelength, as we reported before. Since for a tau protein, there are many surface antigens available for specific recognition with monoclonal anti-tau antibody-conjugated nanoparticles, as shown in Figure 1C, antibody-conjugated gold nanoparticles undergo aggregation in presence of tau protein. Now because of the aggregation in the presence of tau, antibody-conjugated gold nanoparticles lose the center of symmetry, and as a result one can expect a significant amount of electric dipole contribution to the two-photon scattering intensity. Since electric dipole contributes several times higher than that of multipolar moments, we expect two-photon scattering intensity to increase upon the addition of tau.

As shown in Figure 2A, a clear colorimetric change is observed when tau protein was added to

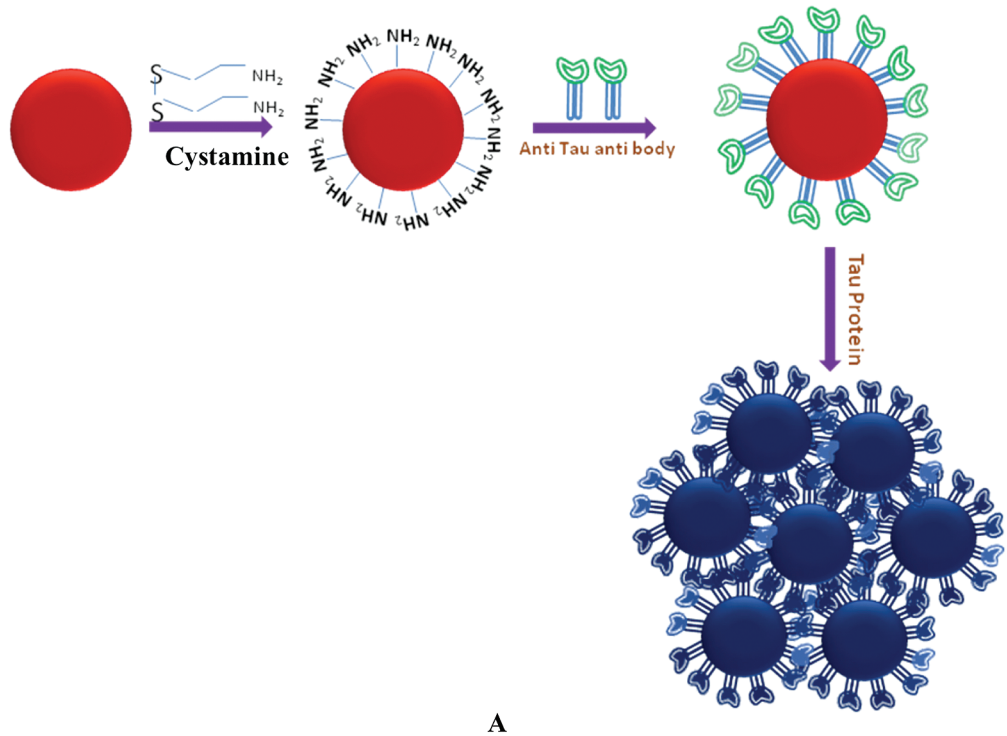

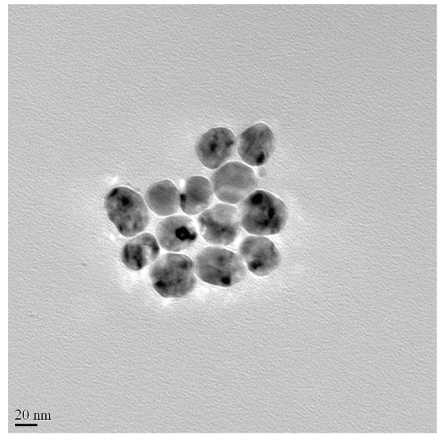

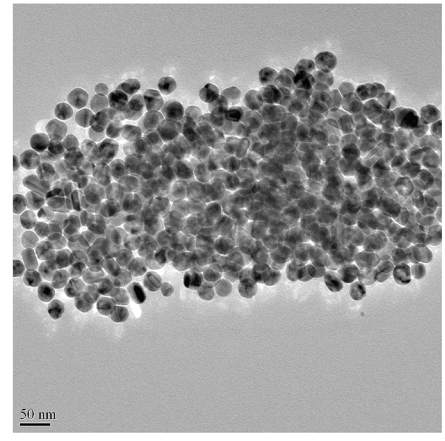

Figure 1. (A) First two steps show schematic representation of the synthesis of monoclonal anti-tau antibody-conjugated gold nanoparticles. Third step shows schematic representation of monoclonal anti-tau antibody-conjugated gold nanoparticle based sensing of tau protein. (B) TEM image of anti-tau antibod-conjugated gold nanoparticles before addition of tau protein. (C) TEM image of anti-tau antibod-conjugated gold nanoparticles after addition of 20 ng/mL tau protein.

anti-tau antibody-conjugated gold nanoparticles. This colorimetric change is mainly due to the aggregation of antibody-conjugated gold nanoparticles, as shown in Figure 1C. We have not observed any color change upon the addition of serum albumin (BSA) protein and heme protein, instead of tau protein to anti-tau antibody-conjugated gold nanoparticles (as shown in Figure 2A). Our TEM data also demonstrated (Figure 2D) that there is no significant aggregation due to the addition of serum albumin (BSA) protein or heme protein to anti-tau antibody-conjugated gold nanoparticles. Figure 2B reports how the absorption maximum for a surface plasmon band of gold nanoparticle at 520 nm changes in the presence of tau, BSA, and heme protein. Our experimental data show that intensity of the absorption band at 520 nm decreases with the addition of 200 ng/mL tau and a new broadband corresponding to the absorption of antibody-conjugated gold nanoparticle aggregates appears at 670 nm. In the same plot, we have also shown that absorption remains about unchanged upon the addition of BSA to anti-tau antibody-conjugated gold nanoparticles. So our colorimetric data demonstrate that our assay is highly sensitive to tau protein, and it can distinguish from BSA, which is one of the most abundant protein components in CSF. Our experimental results also show that tau protein can be de-

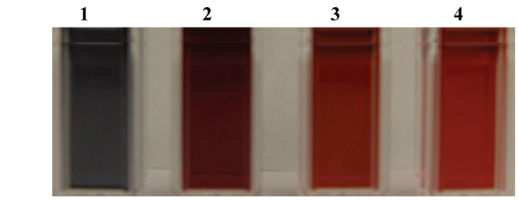

A

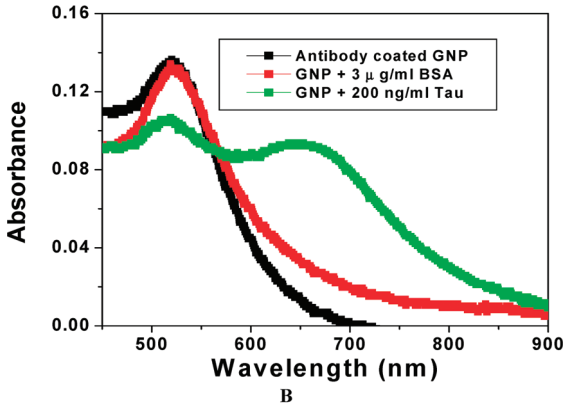

B

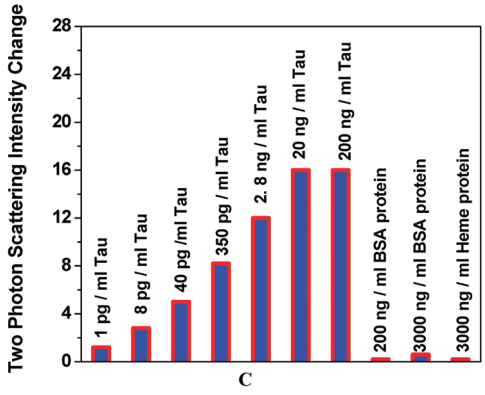

C

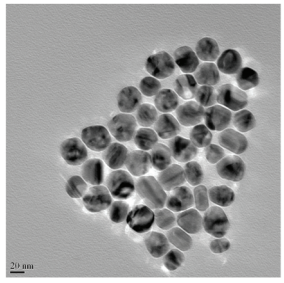

D

Figure 2. (A) Photograph showing colorimetric change upon addition of (1) 200 ng/mL tau, (2) 2.8 ng/mL of tau, (3) 3000 ng /mL BSA protein, (4) 800 mg/mL heme protein. (B) Absorption profile variation of monoclonal anti-tau antibody conjugated gold nanoparticle due to the addition tau protein (200 ng/mL tau). The strong long wavelength band in the visible region (λ_{PR} = 520 nm) is due to the oscillation of the conduction band electrons. A new band appearing around 670 nm, due to the addition of tau protein, demonstrates the aggregation of gold nanoparticles. (C) Plot demonstrating two-photon scattering intensity changes (by 16 times) due to the addition of tau protein to anti-tau antibody conjugated gold nanoparticle. Two-photon scattering intensity changes very little upon addition of BSA and heme protein. (D) TEM image after addition of 800 ng/mL BSA protein, (E) TEM image demonstrating aggregation of anti-tau antibody conjugated gold nanoparticle after the addition of 350 pg/mL tau.

tected in the 2.8 ng/mL level with colorimetric study, whereas TPRS can detect even at 1 pg/mL level. Our experimental results clearly exhibit that TPRS assay can be 3 orders of magnitude more sensitive than the colorimetric assay. Now this new absorption band appearing at 670 nm upon the addition of tau protein can influence the TPRS intensity very highly. According to the two-state model,[48]

$$\beta^{\text{two state}} = \underbrace{\frac{3\mu_{eg}^{2}\Delta\mu_{eg}}{E_{eg}^{2}}}_{\text{static factor}} \underbrace{\frac{\omega_{eg}^{4}}{(\omega_{eg}^{2} - 4\omega^{2})(\omega_{eg}^{2} - \omega^{2})}}_{\text{dispersion factor}} \tag{2}$$

where ω is the fundamental energy of the incident light, μ_{eg} is the transition dipole moment and ω_{eg} is the transition energy between the ground state $\|g\rangle$ and the charge- excited state $\|e\rangle$, $\Delta\mu_{eg}$ is the difference in dipole moment between $\|e\rangle$ and $\|g\rangle$ states. Since $\omega_{eg} \propto 1/\lambda_{max}$, β should change tremendously upon the addition of tau protein and as a result, the two-photon scattering intensity should change tremendously with the addition of tau. So, due to the aggregation after addition of tau protein, the two-photon Rayleigh scattering (TPRS) intensity change observed in our assay, can be due to several factors and these are (1) one can expect significant amount of electric dipole contribution to the two-photon scattering intensity as we discussed before; (2) owing to the change of λ_{max} toward red, TPRS intensity should change after addition of tau protein, as we discussed above; (3) since size increases tremendously with aggregation, the two-photon scattering intensity should increase with the increase in particle size.

To understand the response rate of the TPRS signal upon the addition of tau protein to anti-tau antibody-conjugated gold nanoparticles, we have measured the TPRS intensity at different time intervals, as shown in Figure 3. Our TPRS experimental data indicate that after the addition of 20 ng/mL tau, the TPRS intensity increases by a factor of 8 within 500 s, then increases

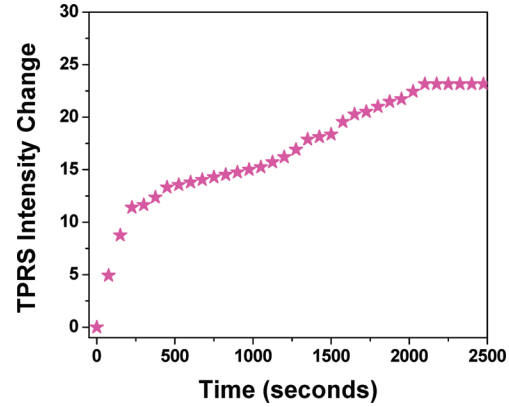

Figure 3. Plot demonstrating the change of TPRS intensity with time, upon the addition of 20 ng/mL tau on anti-tau antibody-conjugated gold nanoparticles.

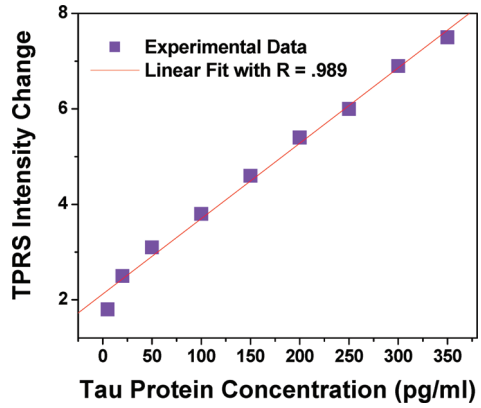

Figure 4. Plot demonstrating linear correlation between two-photon scattering intensity and concentration of tau protein over the range of 5−350 ng/mL with $R = 0.989$.

slowly with time, and then remains constant after 2000 s. Our time interval TPRS intensity measurement indicates that the time frame of our measurement is only half an hour.

To evaluate whether TPRS assay is capable of measuring tau protein concentration quantitatively, we performed two-photon Rayleigh scattering intensity measurements upon the addition of different concentrations of target tau protein to anti-tau antibody-conjugated gold nanoparticles. As shown in Figure 4, the two-photon scattering intensity increment is highly sensitive to the concentration of target tau protein over the range of 5−350 ng/mL and the intensity increased linearly with concentration. Our experimental results also indicate that there is no linear correlation between TPRS intensity and tau protein concentration between 1 and 5 pg/mL and 350−850 pg/mL region.

So our anti-tau antibody-conjugated gold nanoparticle based two-photon scattering assay can provide a quantitative measurement of tau protein concentration over a range of 5−350 ng/mL.

CONCLUSIONS

We have demonstrated for the first time a label-free, fast, and highly sensitive monoclonal anti-tau antibody (tau-mab) coated gold nanoparticle based two-photon scattering assay for the selective detection of Alzheimer's tau protein in a 1 pg/mL level. The detection limit of our TPRS assay is about 2 orders of magnitude lower than cutoff values (195 pg/mL) for tau protein in CSF. We have shown that when anti-tau antibody-coated gold nanoparticle were mixed with 20 pg/mL concentrations of tau protein, two-photon scattering intensity increases by about 16 times. Our experimental data with serum albumin (BSA) protein as well as IgG protein with anti-tau antibody-conjugated gold nanoparticles clearly demonstrated that our TPRS assay is highly sensitive to tau protein and it can distinguish from BSA, which is one of the most abundant protein components in CSF. Our experiment indicates this bioassay is rapid and takes less than 35 min from protein binding to detection and analysis and it can be 3 orders of magnitude more sensitive than the usual colorimetric technique. Our concentration-dependent measurements point out that our antibody-conjugated gold nanosystem based two-photon scattering assay can provide a quantitative measurement of tau protein concentration in the pg/mL region. Our assay will have several advantages: (i) it can be 2 orders of magnitude more sensitive than the usual colorimetric technique and (ii) tau protein can be discriminated very easily from other protein. Our experimental results reported here open up a new possibility of rapid, easy, and reliable diagnosis of AD biomarkers by measuring the TPRS intensity from antibody-modified gold nanosystems.

EXPERIMENTAL METHODS

Hydrogen tetrachloroaurate ($HAuCl_4 \cdot 3H_2O$), $NaBH_4$, buffer solution, NaCl, sodium citrate, monoclonal anti-tau antibody (tau-mab), and tau protein were purchased from Sigma-Aldrich and used without further purification.

Gold Nanoparticle Synthesis. Gold nanoparticles of different sizes and shapes were synthesized by controlling the ratio of $HAuCl_4$, $3H_2O$, and sodium citrate concentration as we reported recently.[16−19,37−39] For smaller gold nanoparticles, we have used a sodium borohydride method as reported before. A 0.5 mL portion of 0.01 M $HAuCl_4$ trihydrate in water and 0.5 mL of 0.01 M sodium citrate in water were added to 18 mL of deionized H_2O and stirred. Next, 0.5 mL of freshly prepared 0.1 M $NaBH_4$ was added, and the solution color changed from colorless to orange. Stirring was stopped, and the solution was left undisturbed for 2 h. The resulting spherical gold nanoparticles were 4 nm in diameter. UV−visible absorption spectrum, colorimetric observation, and transmission electron microscope (TEM) (as shown in Figure 2) were used to characterize the nanoparticles. The particle concentration was measured by UV−visible spectroscopy using the molar extinction coefficients at the wavelength of the maximum absorption of each gold colloid as reported recently [$\varepsilon_{(15)\,518\,nm} = 3.6 \times 10^8\ cm^{-1}\ M^{-1}$.[16−19,37−39]

Preparation of Monoclonal Anti-Tau Antibody (Tau-Mab)-Coated Gold Nanoparticle. For the preparation of monoclonal anti-tau antibody (tau-mab)-conjugated nanoparticles, we have modified the gold nanoparticle surface by amine groups (as shown in Scheme 1) using cystamine dihydrochloride using the reported method.[27,41] For this purpose, we have added 30 mM cystamine dihydrochloride to 50 mL of gold nanoparticle and the solution was kept at 50 °C for several hours under constant sonication. After that, the excess cystamine dihydrochloride was removed by centrifugation at 8000 rpm for several minutes. For covalent immobilization of the monoclonal anti-tau antibody onto the amine-modified gold nanoparticle (GNP) surface, we have used the highly established glutaraldehyde spacer method. In brief, 10 mL of amine-functionilized GNP were incubated with monoclonal anti-tau antibody for 12 h at 4 °C in PBS media. To remove the excess antibody, we have washed monoclonal anti-tau antibody conjugated GNP several times with PBS. During this amine group activation and immobilization of the antibody, we have not noted any aggregation of gold nanoparticles as examined by TEM and UV−vis absorption spectroscopy.

Two-Photon Rayleigh Scattering Spectroscopy. Two-photon Rayleigh scattering (TPRS)[10−19,45−47] from an isotropic solution was observed for the first time in 1965,[10] shortly after the invention of high power ruby lasers. When an intense light of fre-

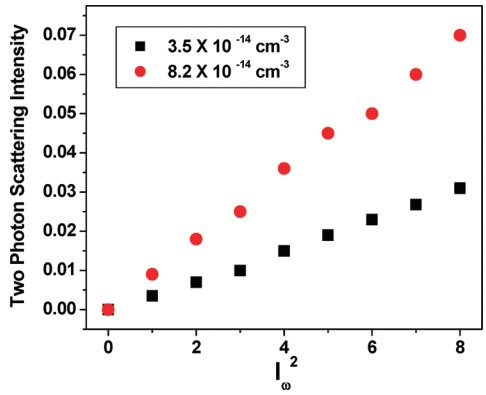

Figure 5. Power dependence of scattering intensity for different concentrations of monoclonal anti-tau antibody-coated gold nanoparticle.

quency ω, is exposed on matter, it can generate a spectrum of the scattered radiation that includes bands with frequency 2ω, due to TPRS, and $2\omega \pm \omega_0$, due to two-photon Raman scattering. In the case of two-photon Raman scattering, ω_0 is the frequency associated with a transition between two energy levels of the scattering molecule. The two-photon light scattering can be observed from fluctuations in symmetry, caused by rotational fluctuations. For the TPRS or HRS experiment, we have used a mode-locked Ti:sapphire laser delivering at fundamental wavelength of 860 nm with a pulse duration of about 150 fs at a repetition rate of 80 MHz. We performed TEM data before and after exposure of about 5−10 min to the laser, and we have not noted any photothermal damage of antibody-coated gold nanoparticles within our HRS data collecting time. The HRS light was separated from its linear counterpart by a high-pass filter and a monochromator, and then detected with a cooled photomultiplier tube. The pulses were counted with a photon counter. The fundamental input beam was linearly polarized, and the input angle of polarization was selected with a rotating half-wave plate. In all experiments reported, the polarization state of the harmonic light was vertical.

Since λ_{max} for monoclonal anti-tau antibody-coated gold nanoparticle (515 nm) and aggregates (650 nm) are very far from the excitation source (860 nm) or second harmonic generated frequency (430 nm), we can eliminate the two-photon luminescence (TPL) contributions in our HRS experiment. To make sure that only a second harmonic signal is collected by PMT, we have used 3 nm interference filter and a monochromator in front of PMT. To understand whether the two-photon scattering intensity at 430 nm light is due to second harmonic generation, we performed power-dependent as well as concentration-dependent studies. Figure 5 shows the output two-photon scattering signal intensities at 430 nm from monoclonal anti-tau antibody-coated gold nanoparticle at different powers of 860 nm incident light. A linear nature of the plot implies that the doubled light is indeed due to the two-photon Rayleigh scattering signal.

Acknowledgment. Dr. Ray thanks NIH-SCORE Grant No. S06GM 008047 and NSF-PREM Grant No. DMR-0611539 for their generous funding. We also thank reviewers whose valuable suggestions improved the quality of the manuscript.

REFERENCES AND NOTES

1. Rookmeyer, R.; Johnson, E.; Ziegler-Graham, K.; Arrighi, M. H. Forcasting the Global Burden of Alzheimer's Disease. *Alzheimer's Dementia.* **2007**, *3*, 186–91.
2. Bu, G. Apolipoprotein E and its Receptors in Alzheimer's Disease: Pathways, Pathogenesis and Therapy. *Nat. Rev. Neurosci.* **2009**, *10*, 333–344.
3. Tanzi, R. E.; Bertram, L. Thirty Years of Alzheimer's Disease Genetics: The Implications of Systematic Meta-Analyses. *Nat. Rev. Neurosci.* **2008**, *9*, 768–778.
4. www.accentonseniors.com/articles/Alzheimers_2008_Fact_Sheet.pdf (accessed Feb 6, 2009).
5. Keating, C. D. Nanoscience Enables Ultrasensitive Detection of Alzheimer's Biomarker. *Proc. Natl. Acad. Sci. U.S.A.* **2005**, *102*, 2263–2264.
6. Georganopoulou, D. G.; Chang, L.; Nam, J.-M.; Thaxton, C. S.; Mufson, E. J.; Klein, W. L.; Mirkin, C. A. Nanoparticle-Based Detection in Cerebro Spinal Fluid of a Soluble Pathogenic Biomarker for Alzheimer's Disease. *Proc. Natl. Acad. Sci. U.S.A.* **2005**, *102*, 2273–2276.
7. Tapiola, T.; Overmyer, M.; Lehtovirta, M.; Helisalmi, S.; Ramberg, J.; Alafuzoff, I. The Level of Cerebrospinal Fluid Tau Correlates with Neurofibrillary Tangles in Alzheimer's Disease. *Neuroreport* **1997**, *8*, 3961–3963.
8. Haes, A. J.; Chang, L.; Klein, W. L.; Van Duyne, R. P. Detection of a Biomarker for Alzheimer's Disease from Synthetic and Clinical Samples Using a Nanoscale Optical Biosensor. *J. Am. Chem. Soc.* **2005**, *127*, 2264–2271.
9. Buerger, K.; Ewers, M.; Pirttila, T.; Zinkowski, R.; Alafuzoff, I.; Teipel, S. J.; DeBernardis, J.; Kerkman, D.; McCulloch, C.; Soininen, H. CSF Phosphorylated Tau Protein Correlates with Neocortical Neurofibrillary Pathology in Alzheimer's Disease. *Brain* **2006**, *129*, 3035–3041.
10. Terhune, R. W.; Maker, P. D.; Savage, C. M. Measurements of Nonlinear Light Scattering. *Phys. Rev. Lett.* **1965**, *14*, 681–684.
11. Clays, K.; Persoons, A. Hyper-Rayleigh Scattering in Solution. *Phys. Rev. Lett.* **1991**, *66*, 2980–3.
12. Antoine, I. R.; Benichou, E.; Bachelier, G.; Jonin, C.; Brevet, P. F. Multipolar Contributions of the Second Harmonic Generation from Silver and Gold Nanoparticle. *J. Phys. Chem. C* **2007**, *111*, 9044–9048.
13. Chandra, M.; Indi, S.; Das, P. K. Depolarized Hyper-Rayleigh Scattering from Copper Nanoparticles. *J. Phys. Chem. C* **2007**, *111*, 10652–10656.
14. Dadap, J. I.; Shan, J.; Eisenthal, K. B.; Heinz, T. F. Second-Harmonic Rayleigh Scattering from a Sphere of Centrosymmetric Materials. *Phys. Rev. Lett.* **1999**, *83*, 4045.
15. Novak, J. P.; Vance, F. W.; Johnson, R. C.; Lemon, B. I.; Hupp, J. T.; Feldheium, D. L. Assembly of Phenylacetylene-Bridged Gold and Silver Nanoparticle Arrays. *J. Am. Chem. Soc.* **2000**, *122*, 12029.
16. Ray, P. C. Label-Free Diagnostics of Single Base-Mismatch DNA Hybridization on Gold Nanoparticles Using Hyper-Rayleigh Scattering Technique. *Angew. Chem., Int. Ed* **2006**, *45*, 1151–1154.
17. Darbha, G. K.; Singh, A. K.; Rai, U. S.; Yu, E.; Yu, H.; Ray, P. C. Highly Selective Detection of Hg^{2+} Ion Using NLO Properties of Gold Nanomaterial. *J. Am. Chem. Soc.* **2008**, *130*, 8038.
18. Darbha, G. K.; Rai, U. S.; Singh, A. K.; Ray, P. C. Gold Nanorod Based Sensing of Sequence Specific HIV-1 Virus DNA Using Hyper Rayleigh Scattering Spectroscopy. *Chem.—Eur. J.* **2008**, *14*, 3896–3903.
19. Griffin, J.; Singh, A. K.; Senapati, D.; Lee, E.; Gaylor, K.; Jones-Boone, J.; Ray, P. C. Sequence Specific HCV-RNA Quantification Using Size Dependent Nonlinear Optical Properties of Gold Nanoparticles. *Small* **2009**, *5*, 839–845.
20. Singh, A K.; Senapati, D.; Wang, S.; Griffin, J.; Neely, A.; Candice, P.; Naylor, K. M.; Varisli, B.; Kalluri, J. R.; Ray, P. C. Gold Nanorod-Based Selective Identification of *Escherichia coli* Bacteria Using Two-Photon Rayleigh Scattering Spectroscopy. *ACS Nano* **2009**, *3*, 1906–1912.
21. Griffin, J.; Singh, A. K.; Senapati, D.; Rhodes, P.; Mitchell, K.; Robinson, B.; Yu, E.; Ray, P. C. Size and Distance Dependent NSET Ruler for Selective Sensing of Hepatitis C Virus RNA. *Chem.—Eur. J.* **2009**, *15*, 342–351.
22. Ni, W.; Kou, X.; Yang, Z.; Wang, J. Tailoring Longitudinal Surface Plasmon Wavelengths, Scattering and Absorption Cross-Sections of Gold Nanorods. *ACS Nano* **2008**, *2*, 677–686.
23. Kumar, R.; Roy, I.; Ohulchanskyy, T. Y.; Goswami, L. N.; Bonoiu, A. C.; Bergey, E. J.; Tramposch, K. M.; Maitra, A.; Prasad, P. N. Covalently Dye-Linked, Surface-Controlled, and Bioconjugated Organically Modified Silica

Nanoparticles as Targeted Probes for Optical Imaging. *ACS Nano* **2008**, *2*, 449–456.
24. Mayer, K. M.; Lee, S.; Liao, H.; Rostro, B. C.; Fuentes, A.; Scully, P. T.; Nehl, C. L.; Hafner, J. H. A Label-Free Immunoassay Based Upon Localized Surface Plasmon Resonance of Gold Nanorods. *ACS Nano* **2008**, *2*, 687–692.
25. Sassolas, A.; Leca-Bouvier, B. D.; Blum, L. J. DNA Biosensors and Microarrays. *Chem. Rev.* **2008**, *108*, 109–139.
26. Wijaya, A.; Schaffer, S. B.; Pallares, I. G.; Kimberly, H.-S. Selective Release of Multiple DNA Oligonucleotides from Gold Nanorods. *ACS Nano* **2009**, *3*, 80–86.
27. Pietrobon, B.; McEachran, M.; Kitaev, V. Synthesis of Size-Controlled Faceted Pentagonal Silver Nanorods with Tunable Plasmonic Properties and Self-Assembly of These Nanorods. *ACS Nano* **2009**, *3*, 21–26.
28. Chou, I.-H.; Benford, M.; Beier, H. T.; Cot, G. L. Nanofluidic Biosensing for β-Amyloid Detection Using Surface Enhanced Raman Spectroscopy. *Nano Lett.* **2008**, *8*, 1729–1735.
29. Vestergaard, M.; Kerman, K.; Kim, D.-K.; Hiep, H. M.; Tamiya, E. Detection of Alzheimer's Tau Protein Using Localised Surface Plasmon Resonance-Based Immunochip. *Talanta* **2008**, *74*, 1038.
30. Zhou, R.; Shi, M.; Chen, X.; Wang, M.; Chen, H. Self-Assembly of Mn-Doped ZnS Quantum Dots/Octa(3-aminopropyl)octasilsequioxane Octahydrochloride Nanohybrids for Optosensing DNA. *Chem.—Eur. J.* **2009**, *15*, 5436–5440.
31. Marbella, L.; Mitasev, B. S.; Basu, P. Development of a Fluorescent Pb^{2+} Sensor. *Angew. Chem., Int. Ed.* **2009**, *48*, 3996–3998.
32. Daniel, W. L.; Han, M. S.; Lee, J. S.; Mirkin, C. A. Colorimetric Nitrite and Nitrate Detection with Gold Nanoparticle Probes and Kinetic End Points. *J. Am. Chem. Soc.* **2009**, *131*, 6362–3.
33. Giljohann, D. A.; Seferos, D. S.; Prigodich, A. E.; Patel, P. C.; Mirkin, C. A. Gene Regulation with Polyvalent siRNA-Nanoparticle Conjugates. *J. Am. Chem. Soc.* **2009**, *131*, 2072–3.
34. Li, Z.; Li, W.; Camargo, P. H. C.; Xia, Y. Fabrication of Two-Dimensional Polymer Arrays: Template Synthesis of Polypyrrole Between Redox-Active Coordination Nanoslits. *Angew. Chem., Int. Ed.* **2008**, *47*, 9886–9889.
35. Donath, E. Biosensors: Viruses for Ultrasensitive Assays. *Nat. Nanotechnol.* **2009**, *4*, 215–216.
36. Zhao, W.; Karp, J. M. Nanoantennas Heat Up. *Nat. Mater.* **2009**, *8*, 453–454.
37. Darbha, G. K.; Ray, A.; Ray, P. C. Gold-Nanoparticle-Based Miniaturized FRET Probe for Rapid and Ultra-Sensitive Detection of Mercury in Soil, Water, and Fish. *ACS Nano* **2007**, *3*, 208–214.
38. Ray, P. C.; Fortner, A.; Darbha, G. K. Gold Nanoparticle Based FRET Asssay for the Detection of DNA Cleavage. *J. Phys. Chem. B* **2006**, *110*, 20745.
39. Singh, A. K.; Griffin, J.; Senapati, D.; Neely, A.; Candice, P.; Naylor, K. M.; Varisli, B.; Kalluri, J. R.; Ray, P. C. Gold Nanorod Based Selective Identification of *Escherichia coli* Bacteria Using Two-Photon Rayleigh Scattering Spectroscopy. *ACS Nano* **2009**, *3*, 1906–1912.
40. Huang, X.; El-Sayed, I. H.; Qian, W.; El-Sayed, M. A. Cancer Cell Imaging and Photothermal Therapy in the Near-Infrared Region by Using Gold Nanorods. *J. Am. Chem. Soc.* **2006**, *128*, 2115–2120.
41. Wang, C.; Irudayaraj, J. Gold Nanorod Probe for the Detection of Multiple Pathogens. *Small* **2008**, *4*, 2004.
42. Tang, B.; Cao, L.; Xu, K.; Zhuo, L.; Ge, J.; Li, Q.; Yu, L. A New Nanobiosensor for Glucose with High Sensitivity and Selectivity in Serum Based on Fluorescence Resonance Energy Transfer (FRET) Between CdTe Quantum Dots and Au Nanoparticles. *Chem.—Eur. J.* **2008**, *14*, 3637.
43. Satyabrata, S.; Mandal, T. K. Tryptophan-Based Peptides to Synthesize Gold and Silver Nanoparticles: A Mechanistic and Kinetic Study. *Chem.—Eur. J.* **2007**, *27*, 3160–3168.
44. Alivisatos, P. The Use of Nanocrystals in Biological Detection. *Nat. Biotechnol.* **2004**, *22*, 47–52.
45. Xiang, J.; Lu, W.; Hu, Y.; Wu, Y.; Yan, H.; Lieber, C. M. High Performance Field Effect Transistors Based on Ge/Si Nanowire Heterostructures. *Nature* **2006**, *441*, 489.
46. Hennrich, G.; Murillo, M. T.; Prados, P.; Al-Saraierh, H.; El-Dali, A.; Thompson, D. W.; Collins, J.; Georghiou, P. E.; Teshome, A.; Asselberghs, I.; *et al*. Alkynyl Expanded Donor-Acceptor Calixarenes: Geometry and Second-Order Nonlinear Optical Properties. *Chem.—Eur. J.* **2007**, *13*, 7753.
47. Duncan, V.; Song, K.; Hung, S-T; Miloradovic, I.; Nayak, A.; Persoons, A.; Verbiest, T.; Therien, M. J.; Clays, K. Molecular Symmetry and Solution-Phase Structure Interrogated by Hyper-Rayleigh Depolarization Measurements: Elaborating Highly Hyperpolarizable D_2-Symmetric Chromophores. *Angew. Chem., Int. Ed.* **2008**, *47*, 2978–2981.
48. Oudar, J. L. Optical Nonlinearities of Conjugated Molecules. Stilbene Derivatives and Highly Polar Aromatic Compounds. *J. Chem. Phys.* **1977**, *67*, 446–457.